

# On the radio properties of the highest redshift quasars

M. Cirasuolo<sup>1</sup>, M. Magliocchetti<sup>2,4</sup>, G. Gentile<sup>2,3</sup>, A. Celotti<sup>2</sup>, S. Cristiani<sup>4</sup>, L. Danese<sup>2</sup>

<sup>1</sup> Institute for Astronomy, University of Edinburgh, Royal Observatory, Edinburgh EH9 3HJ

<sup>2</sup> S.I.S.S.A., Via Beirut 2-4, 34014, Trieste, Italy

<sup>3</sup> University of New Mexico, Dept. of Physics and Astronomy, 800 Yale Blvd Ne, Albuquerque, NM 87131, USA

<sup>4</sup> INAF - Osservatorio Astronomico di Trieste, Via G.B. Tiepolo 11, 40131, Trieste, Italy

6 September 2017

## ABSTRACT

We present deep radio observations of the most distant complete quasar sample drawn from the Sloan Digital Sky Survey. Combining our new data with those from literature we obtain a sample which is  $\sim 100$  per cent complete down to  $S_{1.4\text{GHz}} = 60\mu\text{Jy}$  over the redshift range  $3.8 \leq z \leq 5$ . The fraction of radio detections is relatively high ( $\sim 43$  per cent), similar to what observed locally in bright optical surveys. Even though the combined radio and optical properties of quasars remain overall unchanged from  $z \sim 5$  to the local Universe, there is some evidence for a slight over-abundance of radio-loud sources at the highest redshifts when compared with the lower- $z$  regime.

Exploiting the deep radio VLA observations we present the first attempt to directly derive the radio luminosity function of bright quasars at  $z \gtrsim 4$ . The unique depth – both in radio and optical – allows us to thoroughly explore the population of optically bright FR II quasars up to  $z \sim 5$  and opens a window on the behaviour of the brightest FR I sources. A close investigation of the space density of radio loud quasars also suggests a differential evolution, with the more luminous sources showing a less pronounced cut-off at high  $z$  when compared with the less luminous ones.

**Key words:** galaxies: active - cosmology: observations - radio continuum: quasars

## 1 INTRODUCTION

During the past years, studies of the properties of Active Galactic Nuclei (AGNs) and in particular of their cosmological evolution have become of major relevance within the more general field of galaxy evolution. In fact, it has been found that the properties of the central black hole (BH) are tightly related to those of the host galaxy (e.g. Magorrian et al. 1998; Ferrarese & Merritt 2000; Tremaine et al. 2002; McLure & Dunlop 2004), so that the energetic feedback that AGN activity can release is now a fundamental ingredient in many theoretical models of galaxy formation (Silk & Rees 1998; Fabian 1999; Granato et al. 2001, 2004; Cavaliere & Vittorini 2002; Di Matteo et al. 2005; Cirasuolo et al. 2005b).

Previous studies in the optical and X-rays – bands which are thought to trace the accretion processes onto the central BH – have established quasar and powerful AGN activity to peak at  $z \sim 2$ , with a rapid decline at lower redshifts (e.g. Boyle et al. 2000; Ueda et al. 2003; Croom et al. 2004); on the other hand, the less powerful sources have their major shining phase at  $z \lesssim 1$  (e.g. Ueda et al. 2003; Hasinger et al. 2005). The behaviour of the AGN evolution at higher redshifts has been very uncertain for a long time as the relevant observations were biased by selection effects and only considered very small numbers of objects. The ad-

vent of the recent Sloan Digital Sky Survey (SDSS; Fan et al. 1999, York et al. 2000) has allowed to properly explore the high redshift Universe up to  $z \sim 6$  (Fan et al. 2001a,b; 2004). These studies have confirmed the presence of a cut off in the space density of quasars at  $z \sim 2$ .

Even though AGNs that show radio emission are only a small fraction of the total population (Sramek & Weedman 1980; Condon et al. 1981; Marshall 1987; Miller, Peacock & Mead 1990; Kellermann et al. 1989), they represent an important subsample as the radiation at centimetre wavelengths is unaffected by dust obscuration and reddening. Therefore, studies of the evolution of radio-active AGNs provide a less biased view of the behaviour of massive BHs and accretion processes onto them as a function of cosmic time.

Several studies have addressed the evolutionary trend of radio loud sources from the local Universe up to high  $z$  (Dunlop & Peacock 1990; Toffolatti et al. 1998; Jackson & Wall 1999; De Zotti et al. 2005). Shaver et al. (1996, 1999) argued for a drop in the space density of flat spectrum radio quasars by more than a factor 10 between  $z \sim 2.5$  and  $z \sim 6$ . However, a re-analysis of such sources (Jarvis & Rawlings 2000) suggests a more gradual (factor  $\sim 4$ ) decline, decline which is backed up by the work of Jarvis et al. (2001) on steep spectrum sources in the same redshift interval. A lu-

minosity dependent cut-off, with a decrease in space density less dramatic for the most luminous radio sources, has been claimed by Dunlop (1998) and confirmed by other recent studies (i.e. Vigotti et al. 2003; Cirasuolo et al. 2005a).

Unfortunately, the process(es) responsible for the formation of radio jets that mark the class of radio loud objects are still poorly understood. The mass of the central BH could play an important role in shaping the transition between the population of radio loud (RL) and radio quiet (RQ) AGNs. As recently pointed out by many studies, RL sources seem to have the BHs confined to the upper end of the BH mass function, whereas the BHs in RQ quasars appears to span the full range in BH mass (Laor 2000; McLure & Dunlop 2002; Dunlop et al. 2003; Marziani et al. 2003; McLure & Jarvis 2004; Metcalf & Magliocchetti 2006). Furthermore, the analysis of a large sample of local low luminosity AGNs drawn from SDSS showed the fraction of galaxies hosting a radio-loud AGN to be a strong function of BH and stellar mass (Best et al. 2005). However, the point is still controversial, and some authors claim no evidence for any relation between radio power and mass of the central BH (Oshlack et al. 2002; Ho 2002; Woo & Urry 2002a,b; but see the dissenting view of Jarvis & McLure 2002 and McLure & Jarvis 2004, who ascribe the lack of correlation reported by these latter authors as due to selection effects such as Doppler Beaming and orientation).

In the light of the above discussion, the present work is aimed at exploring the radio properties of the highest redshift quasars. The main goal is to investigate if the physical conditions in the early stages of galaxy formation can favour or prevent the formation of relativistic jets and also to test if the radio loudness in quasars exhibits some dependence on cosmic epoch. For this purpose, we performed deep radio observations of a sample of high redshift quasars selected from SDSS. The optical sample is presented in Section 2, while radio observations and the radio properties of the sample are respectively described in Sections 3 and 4. By exploiting this unique sample we derive the radio luminosity function in Section 5 and investigate the behaviour of the space density of high redshift QSOs as a function of redshift in Section 6. Our discussion and conclusions are presented in Section 7. Throughout this paper we adopt the ‘‘concordance’’ cosmology, consistent with the Wilkinson Microwave Anisotropy Probe data (Bennett et al. 2003), i.e.:  $\Omega_M = 0.3$ ,  $\Omega_\Lambda = 0.7$  and  $H_0 = 70 \text{ km s}^{-1}$ .

## 2 THE SAMPLE

The optical quasar sample we consider in this work was drawn from the Sloan Digital Sky Survey (SDSS) and represents the largest, complete, high-redshift quasar sample to date.

This dataset (Fan et al. 2001a) consists of 39 bright ( $i^* \lesssim 20$ ), high-redshift ( $3.6 \leq z \leq 5$ ) quasars observed in the Fall Equatorial Stripe at high Galactic latitude, covering an area of 182 sq. deg. High redshift quasar candidates were selected using colour cuts by exploiting the five photometric bands ( $u^*, g^*, r^*, i^*, z^*$ ) available from SDSS observations.

The quasar continuum is assumed to be a power law with a slope  $\alpha_o$ , i.e.  $f_\nu \propto \nu^{-\alpha_o}$ . The continuum magnitude,  $AB_{1450}$ , is defined as the rest-frame AB magnitude at  $\lambda =$

1450 Å corrected for Galactic extinction. For a power law continuum, the  $AB_{1450}$  magnitude can be converted into the rest-frame Kron-Cousins B band magnitude:

$$B = AB_{1450} + 2.5\alpha_o \log(4400/1450) + 0.12, \quad (1)$$

where 4400 Å is the effective wavelength of the B band filter, and the factor 0.12 is the zeropoint difference between the AB magnitude system and the Vega-based system (Schmidt et al. 1995).

The mean optical spectral index for the sources in the sample is  $\alpha_o = 0.79$  (Fan et al. 2001a), even though Pentericci et al. (2003) – making use of near-IR observations (J, H and K band) – found a slightly flatter slope,  $\alpha_o \sim 0.5$ .

Due to the optical limit  $i^* \lesssim 20$  adopted to select these sources, the final sample is only representative of bright quasars with absolute magnitudes in the range  $-28.5 \lesssim M_B \lesssim -26$ .

## 3 VLA OBSERVATIONS

Out of the 39 quasars which form the optical sample, 5 of them have radio counterparts in the FIRST (Faint Images of the Radio Sky at 20 cm) survey (Becker, White & Helfand 1995) with relatively high 1.4 GHz fluxes:  $1.4 \lesssim S_{1.4\text{GHz}} (\text{mJy}) \lesssim 10$ . These sources have an offset between radio and optical positions of less than 0.4 arcsec, except for the faintest one (J2322-0052) which has an offset of 0.8 arcsec, still compatible with the positional accuracy of 1 arcsec of the FIRST survey for fluxes  $\sim 1 \text{ mJy}$ . Their structure is point-like, except for J0210-0018 which is the brightest of our objects at 1.4 GHz with  $S_{1.4\text{GHz}} = 9.75 \pm 0.1 \text{ mJy}$ ; the FIRST image of this source reveals a small component with a flux of 2 mJy at a distance of 10 arcsec from the centre of the optical position, probably indicating the presence of an extended structure (with a proper linear size of  $\sim 65 \text{ kpc}$ ).

Other 15 sources of the original Fan et al. (2001a) sample were observed by Carilli et al. (2001), as a part of an extensive program on high redshift quasars at radio wavelengths. These sources were observed at 1.4 GHz for  $\sim 2$  hours each, reaching a theoretical rms noise ( $\sigma_{\text{rms}}$ ) of the order of  $20 - 30 \mu\text{Jy}$ . Only 4 sources were detected at  $> 3\sigma_{\text{rms}}$  and other 3 sources at  $2.5 \leq \sigma_{\text{rms}} \leq 3$ . Considering the exact coincidence of the radio positions with the optical ones, in the following analysis we will take as true detections even these latter three sources with  $> 2.5\sigma_{\text{rms}}$ .

In order to constrain the radio properties of the whole optically selected sample, we then performed deep 1.4 GHz observations with the Very Large Array (VLA) of the remaining 19 sources. These observations were made in the BnA configuration in October 2003 and January 2004; the correlator setup was such that the total bandwidth was 100 MHz with two orthogonal polarizations. Every source was observed for about 2 hours, divided into short scans spanning a large range in hour angle, in order to have a reasonably good coverage of the u-v plane. The data reduction and analysis were performed within AIPS; standard phase and amplitude calibration were applied, and subsequently these were refined with self-calibration using background sources in the field of view. The dirty maps were cleaned and then restored using Gaussian beams of about 5 arcsec. The theoretical noise level has been roughly achieved in most of

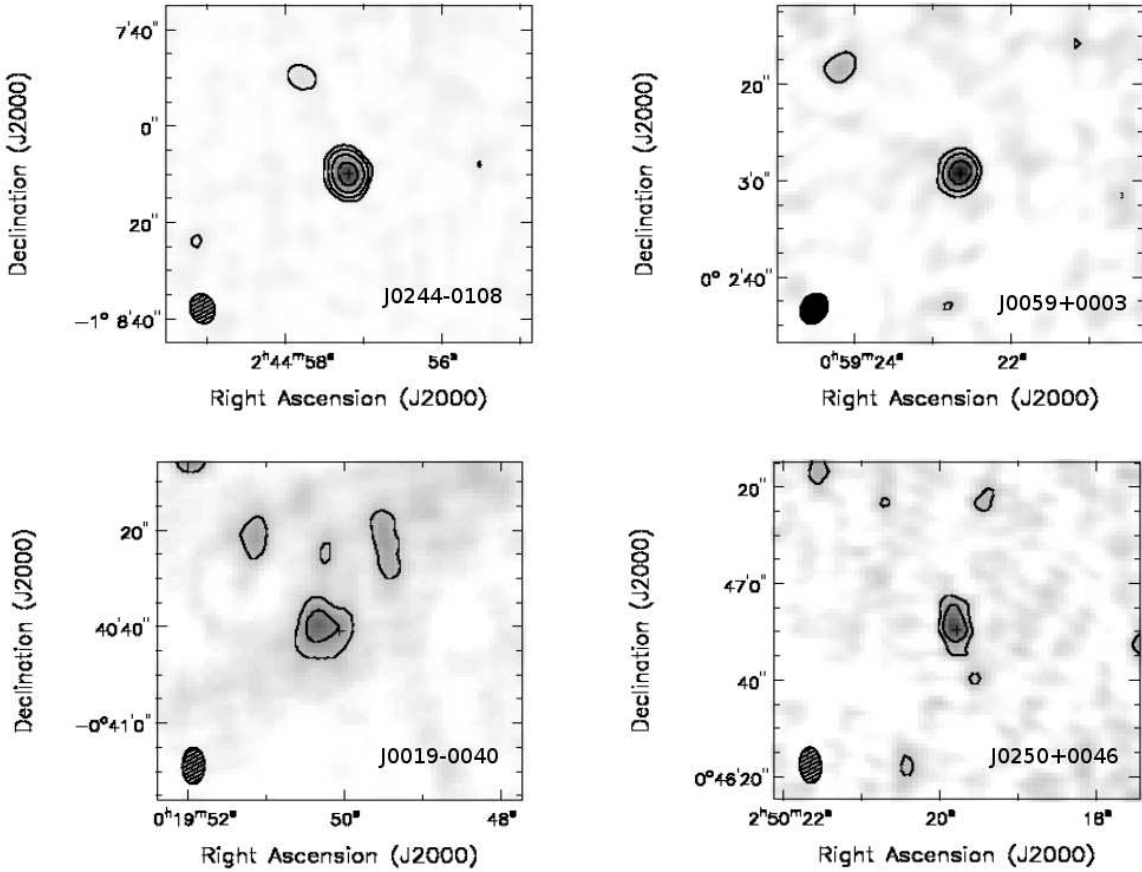


**Figure 1.** Images at 1.4 GHz of the 4 high redshift quasars detected at  $> 3\sigma_{\text{rms}}$ . The FWHM of the Gaussian restoring beams are shown in the corners of all frames.

the sources, except for J2306+0108 ( $\sigma_{\text{rms}} = 65 \mu\text{Jy}$ ) due to side-lobe confusion by a bright source in the field.

Four quasars (see Figure 1) have been detected at  $> 3\sigma_{\text{rms}}$ . Two of these sources, J0244-0108 and J0059+0003, are relatively bright ( $S_{1.4\text{GHz}} = 612 \pm 20 \mu\text{Jy}$  and  $S_{1.4\text{GHz}} = 461 \pm 29 \mu\text{Jy}$ , respectively), while the other two have fluxes in the range  $150 \lesssim S_{1.4\text{GHz}} (\mu\text{Jy}) \lesssim 180$  (see Table 1). Another source (J0204-0112) has been detected at  $\sim 2.5 \sigma_{\text{rms}}$  with a flux  $S_{1.4\text{GHz}} = 53 \pm 20 \mu\text{Jy}$ . The remaining 14 sources are undetected and their fluxes will be treated as upper limits in the following analysis.

#### 4 REDSHIFT DISTRIBUTION AND COMPLETENESS

Combining our VLA observations with the ones made by Carilli et al. (2001) and with the information stemming from FIRST we obtain 17 radio detections out of the 39 quasars ( $\sim 43$  per cent) constituting the whole optical sample.

The redshift distribution of these radio-detected sources is shown in Figure 2 as a solid histogram. For a comparison, Figure 2 also shows the redshift distribution of the 39 quasars of the optical sample. It is worth noting that the fraction of radio detections is relatively high ( $\sim 40$  per cent) at  $z \gtrsim 3.8$  but it drops to  $\sim 10$  per cent in the redshift range

$3.6 \lesssim z \lesssim 3.8$ . We are not aware of any specific selection effect that can justify this rather peculiar trend. One possible cause of such finding would be a significant contamination of the sample by young radio sources, whose spectrum can be inverted up to tens of GHz and whose density is expected to increase at higher redshifts.

Despite the results of a Kolmogorov-Smirnov (KS) test, which show that the redshift distribution of radio detected sources and that of the underlying parent population are not statistically different ( $P_{\text{KS}} \sim 0.3$ ), in order to avoid any unforeseen bias in our analysis, in the following we will always discuss results obtained for  $z \gtrsim 3.8$  and only comment on the effects of including sources from the  $3.6 \lesssim z \lesssim 3.8$  bin.

As shown in Figure 3, the radio follow up of the optical sample in the range  $3.8 \lesssim z \lesssim 5$  is nearly complete down to  $S_{1.4\text{GHz}} \sim 60 \mu\text{Jy}$ . The only exception is a single upper limit for the source J2309-0031 from Carilli et al. (2001), which has a  $2\sigma$  detection at  $S_{1.4\text{GHz}} = 88 \pm 44 \mu\text{Jy}$  with relatively high noise. Only one detected source (J0204-0112) lies under the flux limit of  $S_{1.4\text{GHz}} \sim 60 \mu\text{Jy}$  and it is our less secure detection at a  $2.5\sigma$  level. Note that pushing the limit down to  $z \lesssim 3.8$  would have the advantage of including another source with  $S_{1.4\text{GHz}} > 60 \mu\text{Jy}$ , but would imply dealing with three more upper limits rather than true detections.

The radio flux limit of  $S_{1.4\text{GHz}} \sim 60 \mu\text{Jy}$  allows to reach completeness down to  $\log_{10} P_{1.4\text{GHz}} \sim 23.6$

Source SDSS	$z$	$AB_{1450}$	$M_{1450}$	$\alpha_o$	$S_{1.4\text{GHz}}$ ( $\mu\text{Jy}$ )
J001950.06-004040.9	4.32	19.62	-26.36	-0.02	$146 \pm 39$
J005922.65+000301.4	4.16	19.30	-26.62	-1.09	$461 \pm 29$
J010822.70+001147.9	3.71	19.62	-26.12	-0.19	$<66 \pm 33$
J012019.99+000735.5	4.08	19.96	-25.93	-0.52	$<40 \pm 20$
J012700.69-004559.1	4.06	18.28	-27.60	-0.66	$<42 \pm 21$
J020427.81-011239.6	3.91	19.80	-26.02	-0.83	$53 \pm 20$
J020731.68+010348.9	3.85	20.10	-25.70	-1.00	$<42 \pm 21$
J023908.98-002121.5	3.74	19.60	-26.15	-0.78	$<42 \pm 21$
J024457.19-010809.9	3.96	18.46	-27.38	-1.21	$612 \pm 20$
J025019.78+004650.3	4.76	19.64	-26.49	-0.59	$179 \pm 19$
J030707.46-001601.4	3.70	20.04	-25.69	-0.71	$<36 \pm 18$
J031036.85+005521.7	3.77	19.25	-26.51	-0.64	$<36 \pm 18$
J033910.53-003009.2	3.74	19.93	-25.82	-1.17	$<38 \pm 19$
J035214.33-001941.1	4.18	19.51	-26.42	-0.16	$<40 \pm 20$
J225452.88+004822.7	3.69	20.24	-25.49	-1.51	$<38 \pm 19$
J225529.09-003433.4	4.08	20.26	-25.63	-1.15	$<46 \pm 23$
J230323.77+001615.2	3.68	20.24	-25.48	-0.77	$<38 \pm 19$
J230639.65+010855.2	3.64	19.14	-26.57	-1.38	$<130 \pm 65$
J235053.55-004810.3	3.85	19.80	-26.00	-0.89	$<56 \pm 28$

**Table 1.** Properties of the 19 quasars observed at 1.4 GHz with the VLA. Redshift and optical data are from Fan et al. (2001a). Upper limits to the undetected sources have been defined as  $S_{1.4\text{GHz}} = 2\sigma_{\text{rms}}$ .

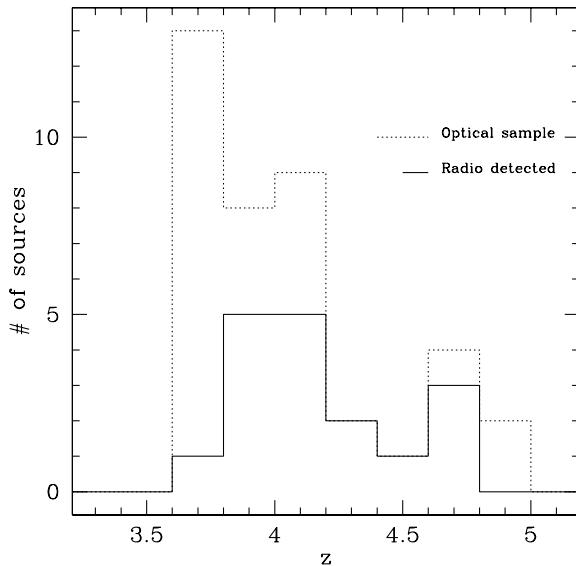


**Figure 2.** Redshift distribution for the radio detected quasars (solid histogram) compared with the one for the 39 sources in the Fan et al. (2001a) dataset (dotted histogram).

$\text{W Hz}^{-1} \text{ sr}^{-1}$  over the entire redshift range considered in this work. This threshold in radio power of course depends on the adopted radio spectral index<sup>\*</sup>,  $\alpha_R$ . Unfortunately, to our knowledge no quasar of the Fan et al. (2001a) sample was observed at radio frequencies other than 1.4 GHz. We were therefore unable to directly measure the radio spectral index of the sources in our sample and in the following analysis the

\* Throughout this work the radio flux density is defined as  $S_\nu \propto \nu^{-\alpha_R}$ .

value  $\alpha_R = 0.5$  has been adopted. Since in the considered redshift range observations at 1.4 GHz select the rest frame spectrum where the flat core component dominates ( $\sim 8$  GHz), it is possible that these high- $z$  sources have a rather flatter radio spectral index than what assumed. The effects of the adoption of a flatter radio spectral index (i.e.  $\alpha_R = 0$ ) on our results will be discussed throughout this paper.

It is also interesting to look at the combined radio and optical properties of these high  $z$  quasars. In Figure 4 the distribution of radio-to-optical ratios<sup>†</sup> ( $R_{1.4}^*$ ) for the radio detected sources in the high redshift sample is shown as a solid histogram while the one derived by using the upper limits is shown as a dotted line. For a comparison, we also plotted as a dashed line the  $R_{1.4}^*$  distribution obtained by Cirasuolo et al. (2003b) for quasars with  $z \lesssim 2$ , renormalized to match the number of sources in our sample. Qualitatively, there is an overall agreement between the  $R_{1.4}^*$  distributions at high and low redshifts, at least for  $R_{1.4}^* \lesssim 10$ ; both distributions show a region of steep transition between the RL and RQ regime. This statement is also confirmed by the KS test which gives high probability  $P_{KS} \gtrsim 0.6$  that the two distributions are not significantly different. In the radio loud regime, instead, there is some evidence for an excess of RL sources in the high- $z$  dataset. In fact, there are 5 sources with  $S_{1.4\text{GHz}} \geq 1 \text{ mJy}$  in such RL tail: two of them have  $R_{1.4}^* \sim 10$ , close to the RL/RQ transition region and the other 3 have  $R_{1.4}^* \gtrsim 100$ . By using the  $R_{1.4\text{GHz}}^*$  distribution from Cirasuolo et al. the expected number of sources with  $R_{1.4}^* \gtrsim 10$  (and  $S_{1.4\text{GHz}} \geq 1 \text{ mJy}$ ) in the same range of redshift and luminosity is  $\sim 2$ , suggesting an overabundance of RL sources at the highest  $z$ . However, due to the limited statistics (only 5 detected objects), the former

† The  $R_{1.4}^*$  parameter is defined as the ratio between the rest frame radio luminosity at 1.4 GHz and the optical luminosity in the B band.

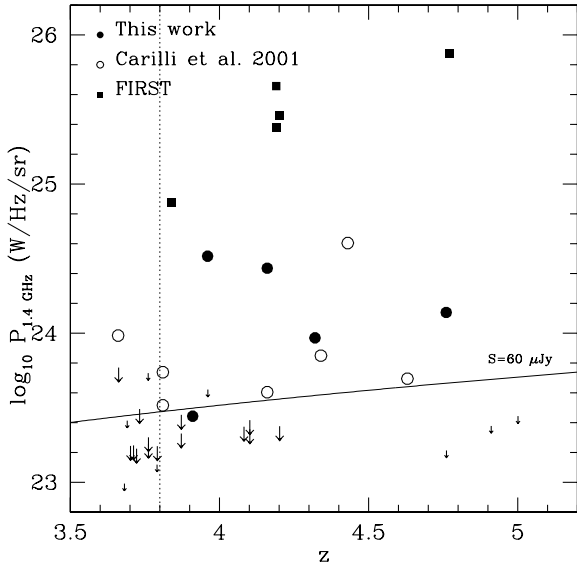


**Figure 3.** Redshift versus radio power for the 39 sources in the complete sample. Filled circles show detections obtained from this work, open circles are from Carilli et al. (2001) and filled squares are detections from FIRST. Long and short down arrows represent upper limits from this work and from Carilli et al. (2001), respectively. The solid line describes the selection effect due to a radio flux limit  $S_{1.4\text{GHz}} = 60 \mu\text{Jy}$ , while the vertical line shows the cut at  $z = 3.8$  (see text for details).

estimate is still compatible with the observed number figures. In fact, a KS test applied between the distribution of RL sources ( $R_{1.4}^* \geq 10$ ) at  $z \gtrsim 4$  and that obtained at lower redshifts gives probabilities  $0.2 \lesssim P_{KS} \lesssim 0.5$  (depending on the adopted value of  $\alpha_R$ ) suggesting that the two distributions are not statistically different. This result remains unchanged even if – in order to increase the statistics – lower values of the radio-to-optical ratios ( $R_{1.4}^* \geq 2-3$ ) are considered. Therefore, even if there is some evidence for an excess of radio-loud sources at high  $z$ , we cannot make any strong statement. Larger samples are definitely needed to clarify this issue.

## 5 LUMINOSITY FUNCTION

Even though small, the sample of radio detected quasars described in the previous Section is sufficient to perform some statistical studies and derive for the first time an estimate of the radio luminosity function (RLF) of optically selected quasars at high redshift. By considering both the optical and radio completeness limits of the sample ( $i^* \lesssim 20$  and  $S_{1.4\text{GHz}} \geq 60 \mu\text{Jy}$ , respectively), we can derive the RLF by using the classical  $1/V_{\text{max}}$  method (Schmidt 1968). For each source we evaluated the maximum redshift at which it could have been included in the sample,  $z_{\text{max}} = \min(z_{\text{max}}^{\text{R}}, z_{\text{max}}^{\text{O}})$ , where  $z_{\text{max}}^{\text{R}}$  and  $z_{\text{max}}^{\text{O}}$  respectively correspond to the values implied by the radio or the optical limiting flux densities. The incompleteness related to the optical multicolour selection has been taken into account by applying to each object in the sample a detection probability as provided by Fan et

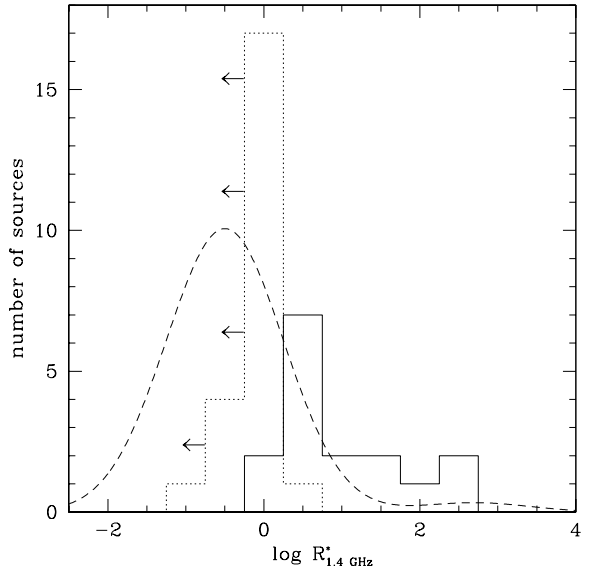


**Figure 4.** Distribution of radio-to-optical ratios for radio detected sources (solid histogram) and undetected ones (dotted histogram), for which upper limits in radio power have been used. The dashed line is the  $R_{1.4}^*$  distribution.

$\log_{10} P_{1.4\text{GHz}}$ (W Hz $^{-1}$ sr $^{-1}$ )	$\log_{10} \phi(P)$ (Mpc $^{-3} \Delta \log_{10} P^{-1}$ )
23.9	$-8.03^{+0.14}_{-0.21}$
24.6	$-8.12^{+0.18}_{-0.30}$
25.3	$-8.40^{+0.23}_{-0.53}$
26.0	$-8.87^{+0.23}_{-0.53}$

**Table 2.** Binned radio luminosity function in the range  $3.8 \leq z \leq 5$  for  $\Omega_m = 0.3$ ,  $\Omega_\Lambda = 0.7$  and  $H_0 = 70 \text{ km s}^{-1} \text{ Mpc}^{-1}$ , as plotted in Figure 5.

al. (2001a) and used by Fan et al. (2001b) to compute the optical luminosity function.

Figure 5 shows the RLF obtained via the  $1/V_{\text{max}}$  method for sources with  $S_{1.4\text{GHz}} \geq 60 \mu\text{Jy}$  in the redshift range  $3.8 \leq z \leq 5$  (see also Table 2). As described in the previous Section, within this redshift range the radio follow-up is almost complete with the exception of a single upper limit. In order to test the reliability of our estimate of the RLF, we then re-computed it by assuming this upper limit to be a real detection. We find that the above assumption only affects the RLF in a negligible way as only the faintest bin changes by a factor less than 5 per cent. This gives us evidence for the stability of our results. We also computed the RLF assuming a flatter radio spectral index ( $\alpha_R = 0$ ). The main effect is to translate the RLF towards lower radio powers by a factor  $\sim 2.5$  without affecting its shape, since the determination of the maximum accessible volume ( $V_{\text{max}}$ ) is driven by the optical cut.

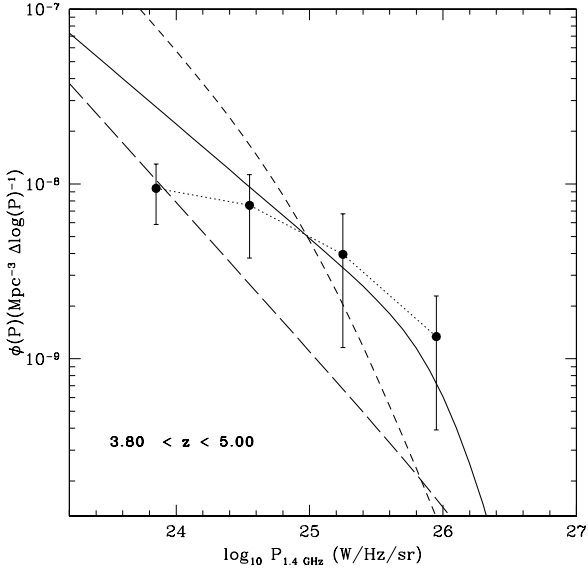


**Figure 5.** Radio luminosity function for sources in the range  $3.8 \leq z \leq 5$  with  $S_{1.4\text{GHz}} \geq 60 \mu\text{Jy}$  (solid dots). For a comparison, as a solid line we show the RLF obtained by De Zotti et al. (2005) for flat spectrum radio quasars, calculated at the mean  $z$  of the bin. Short dashed and long dashed curves illustrate the RLFs obtained by Dunlop & Peacock (1990) for flat spectrum radio sources by respectively assuming a pure luminosity evolution and a luminosity dependent evolution model.

For a comparison, Figure 5 also shows the high  $z$  extrapolation of the RLF for flat spectrum radio quasars as recently inferred by De Zotti et al. (2005). The evolutionary model derived by De Zotti et al. for the population of radio sources has been obtained by fitting number counts and redshift distributions of several radio selected samples at different frequencies. An overall good agreement between our determination of the RLF and the one derived by De Zotti et al. (2005) is found over about two decades in radio luminosity.

In Figure 5 we also compare our RLF estimates with the predictions by Dunlop & Peacock (1990) for flat spectrum radio sources. The dashed and long dashed curves show the RLFs obtained by respectively assuming a pure luminosity evolution and a luminosity dependent evolution model, translated to the concordance cosmology adopted in this paper. We note a moderate agreement with observations only for  $\log_{10} P_{1.4\text{GHz}} \lesssim 25 \text{ W Hz}^{-1} \text{ sr}^{-1}$  in the case of luminosity dependent evolution of radio sources. However, it is worth noticing that the Dunlop & Peacock RLFs are completely unconstrained at these high redshifts, so they have to be merely considered as a pure extrapolation.

It is however important to notice that a direct comparison between the RLF obtained from our high redshift quasars and models for the different radio populations as derived by De Zotti et al. (2005) or Dunlop & Peacock (1990) is not straightforward. These models in fact include all the radio sources regardless of their optical properties, while our RLF is only representative of bright ( $M_B < -26.5$ ) optical quasars. For a meaningful data-to-model comparison we should then take into account the (unknown) contribution

from fainter FRII sources and quasars. The problem is however not as bad as it looks since – as Cirasuolo et al. (2003b) have shown – even though with a large scatter, optical and radio luminosities are broadly correlated so that the contribution of these “missing” faint sources should typically affect the RLF at luminosities lower than those probed by our work.

As we will discuss in more detail in Section 6, we have also compared our findings with extrapolations of the RLF obtained at lower  $z$  by Cirasuolo et al. (2005a) and Willott et al. (2001). These extrapolations are not able to reproduce the high redshift data presented in this paper since they assume a negative evolution which is too quick for  $z \gtrsim 2-3$ .

## 6 SPACE DENSITY

The number of quasars in our sample only allowed us to compute the RLF in a single redshift bin. Moreover, as described in the previous Section, comparisons with evolutionary models for the different radio populations is biased by the bright optical cut in our sample and the lack of information on the radio spectral indices. Therefore, the best way to explore the cosmological evolution of radio quasars and shed light on the behaviour of radio loudness up to the highest accessible redshifts is to look at the evolution of an integrated quantity such as their space density.

Figure 6 shows the comparison between space densities of radio quasars as computed at different redshifts and for different ranges of optical luminosities. The solid square in the Figure represents the space density obtained from the high redshift sample ( $3.8 \leq z \leq 5$ ) presented in this work by considering sources with  $M_B \leq -26.5$  and  $\log_{10} P_{1.4\text{GHz}} \geq 24.4 \text{ W Hz}^{-1} \text{ sr}^{-1}$ . The optical cut is due to the apparent magnitude limit  $i^* \lesssim 20$  of the optical sample. The cut in radio power has instead been chosen in order to have an unbiased comparison with the space densities computed at lower redshifts. For  $z \lesssim 2.2$ , the space density was derived by using a combined sample from the 2dF Quasar Redshift Survey (Croom et al. 2004) and the Large Bright Quasar Survey (LBQS; Hewett et al. 1995). Both these surveys have been cross-correlated with the FIRST dataset (Cirasuolo et al. 2003a, 2005; Hewett et al. 2001) in order to obtain samples of quasars complete in radio down to a flux limit of  $S_{1.4\text{GHz}} = 1 \text{ mJy}$ , which translates into  $\log_{10} P_{1.4\text{GHz}} \gtrsim 24.4 \text{ W Hz}^{-1} \text{ sr}^{-1}$  at  $z \lesssim 2.2$  (open circles). In order to minimize selection effects in the comparison of the space densities of high and low redshift quasars, we then applied to the low redshift sample the same optical ( $M_B \leq -26.5$ ) cut of the  $z \simeq 4$  dataset. It is worth noting that some selection effects can arise from the different selection techniques applied to construct the 2dF-LBQS samples and that of SDSS quasars. However, at the bright magnitudes considered in this paper these effects should be negligible.

The filled dots in Figure 6 show the space density obtained from the combined 2dF-LBQS-FIRST sample as described above. It is clear from the Figure that the drop in the space density of optically bright RL quasars between  $z \sim 2$  and  $z \sim 4.4$  is not very pronounced although errors are large. This result remains mostly unchanged when the space density is computed over the entire redshift range

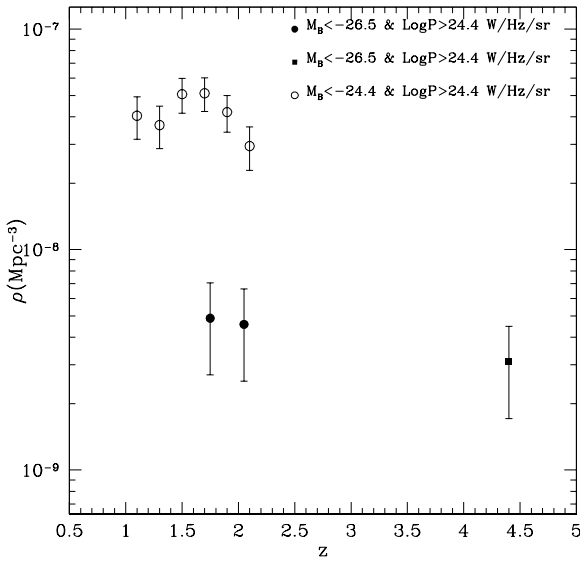


**Figure 6.** Space density of radio quasars with  $\log_{10}P_{1.4\text{GHz}} \geq 24.4 \text{ W Hz}^{-1} \text{ sr}^{-1}$  computed at different redshifts and for different optical luminosities (see text for details). The filled square represents the space density for those sources in the high redshift sample ( $3.8 \leq z \leq 5$ ) presented in this paper ( $M_B \leq -26.5$ ), while the filled dots show the space density for the combined 2dF-LBQS-FIRST sample at lower redshifts derived by applying the same optical and radio cuts as above. The space density of optically fainter sources ( $M_B \leq -24.4$ ) from the combined 2dF-LBQS-FIRST sample as obtained by Cirasuolo et al. (2005) is shown at the different redshifts as open circles.

$3.6 \leq z \leq 5$ . In fact, no other source with  $\log_{10}P_{1.4\text{GHz}} \geq 24.4 \text{ W Hz}^{-1} \text{ sr}^{-1}$  is present in the range  $3.6 \leq z \leq 3.8$ , and the effect of sampling a slightly larger volume is minimal.

To quantify the decline in the space density of optically bright radio quasars we apply a linear regression to the three data points with  $M_B < -26.5$ , obtaining a value for the slope of  $-0.07 \pm 0.11$ , entirely consistent with no evolution. If we instead use a flatter radio spectral index ( $\alpha_R \sim 0$ ) for the high redshift sources, the space density at  $z \sim 4.4$  drops by a factor  $\sim 1.5$  leading to a slightly steeper slope of  $-0.14 \pm 0.13$ . Therefore, we conclude that, independent of the adopted radio spectral index, the drop in the space density of optically bright RL quasars between  $z \sim 2$  and  $z \sim 4.4$  is at most a factor  $\sim 1.5 - 2$ .

The above trend is in agreement with recent results from Vigotti et al. (2003). By using a sample of 13 radio quasars, these authors showed the decline in their space density to be approximately a factor 2 between  $z \sim 2$  and 4. This is close to our findings, even though the objects used by Vigotti et al. (2003) are about one magnitude brighter in optical ( $M_B \lesssim -27.5$ ) than those in our sample, while the radio selection in the two datasets is roughly the same ( $\log_{10}P_{1.4\text{GHz}} > 24.6 \text{ W Hz}^{-1} \text{ sr}^{-1}$ ).

It is interesting to note that the behaviour of bright quasars seems to differ from that of fainter sources which instead present a sharper decline toward higher redshifts. Figure 6 shows (open circles) the space density at low redshifts ( $z \lesssim 2.2$ ) of fainter ( $M_B \leq -24.4$ , completeness limit

of the combined 2dF-LBQS-FIRST dataset for  $z \lesssim 2.2$ ) optical quasars. As already pointed out by Cirasuolo et al. (2005a), this space density shows a decrement of a factor  $\sim 2$  already in the narrow redshift range  $z \sim 1.7$  and  $z \sim 2.2$ . In fact, by fitting with a straight line the values of the space density at  $z \geq 1.7$  we find a slope of  $-0.6 \pm 0.3$ . This trend, when compared with the behaviour of the optically brighter sources which only show a moderate decline up to  $z \sim 4.4$ , is suggestive of a differential evolution of radio-active sources of different optical luminosities. Certainly, the lack of information on the space density of fainter sources at higher redshifts ( $z \gtrsim 2.2$ ) does not allow any definitive conclusion, but our results indicate the cosmological evolution of radio activity in quasars to be a function of their optical power.

## 7 DISCUSSION AND CONCLUSIONS

We have presented deep radio observations of the most distant complete quasar sample drawn from the Sloan Digital Sky Survey. Combining our deep VLA observations with the ones performed by Carilli et al. (2001) and also with the 5 detections from FIRST, we obtained  $\sim 100$  per cent completeness down to  $S_{1.4\text{GHz}} = 60 \mu\text{Jy}$  over the redshift range  $3.8 \leq z \leq 5$ .

The fraction of radio detections is relatively high ( $\sim 43$  per cent), similar to what observed locally for bright optical surveys such as the Palomar Bright Quasar Survey (Kellermann et al. 1989) and the LBQS (Hewett et al. 2001). A comparison between the  $R_{1.4}^*$  distribution of these high redshift radio quasars with the one derived at  $z \lesssim 2$  by Cirasuolo et al. (2003b) suggests that the combined radio and optical properties of quasars might remain overall unchanged from  $z \sim 5$  to the local Universe. However, even though the shape of the  $R_{1.4}^*$  distribution is roughly preserved over cosmic time, there is some marginal evidence for a slight over-abundance of radio loud sources at high  $z$  when compared with the low redshift samples (see Figure 4), even though not statistically significant due to the small number of sources. Furthermore, it is worth noting that the adoption of a flatter  $\alpha_R$  for high  $z$  objects would reduce their radio power and shift them towards lower values of  $R_{1.4}^*$ , therefore somehow reducing the fraction of purely RL ( $R_{1.4}^*$ ) sources.

An interesting hint to shed some light on the above issue comes from comparisons with the parent optical population. The space density of bright optical quasars ( $M_B < -26.5$ ) at  $z \sim 2$  and  $z \sim 4.4$  is  $\rho_O \sim 2 \times 10^{-7} \text{ Mpc}^{-3}$  and  $\rho_O \sim 1.5 \times 10^{-8} \text{ Mpc}^{-3}$ , respectively (see Fan et al. 2001b, 2004). The ratio between the space densities of radio sources with  $\log_{10}P_{1.4\text{GHz}} \geq 24.4 \text{ W Hz}^{-1} \text{ sr}^{-1}$  (as plotted in Figure 6) and the  $\rho_O$  of the total optical population is therefore  $0.025 \pm 0.01$  at  $z \sim 2$  and  $0.15 \pm 0.1$  at  $z \sim 4.4$ . These figures have been obtained for a radio spectral index  $\alpha_R = 0.5$  but, as shown in section 6, the results are not expected to exhibit great variations by adopting a flatter slope. Again, this suggests that at high redshifts the probability of having RL sources is enhanced with respect to that at lower redshifts. However, we stress once more that the statistics we dealt with in this work is very poor and further data and larger samples are needed in order to have a more robust answer.

Even though a detailed investigation of this phenomenon is

outside the possibility of the present data, in a very qualitative way we can relate the suggested excess of RL sources at high  $z$  as compared with the lower redshift regime with changes in the accretion rates with cosmic time. The physical conditions of the primordial massive galaxies hosting quasars and the availability of a larger amount of gas in these early stages could in fact allow super-Eddington accretions and eventually favour the formation of powerful radio jets.

We also attempted the first direct estimate of the radio luminosity function of bright quasars at  $z \gtrsim 4$ . Exploiting the deep radio flux limits obtained through VLA observations, we were able to trace the RLF down to  $\log_{10} P_{1.4\text{GHz}} \sim 23.6 \text{ W Hz}^{-1} \text{ sr}^{-1}$ . It is worth noticing that the transition region between the FR I and FR II population occurs at  $\log_{10} P_{1.4\text{GHz}} \sim 24.4 \text{ W Hz}^{-1} \text{ sr}^{-1}$ . Therefore, the unique depth – both in radio and optical – of this high redshift quasar sample allows us to completely explore the population of optically bright FR II quasars up to  $z \sim 5$  and furthermore opens a window on the behaviour of the brightest FR I sources.

Finally, close investigation of the RL quasar space density at different redshifts is suggestive of a differential evolution for the two populations of optically faint and bright objects. The more luminous sources in fact show a less pronounced cut-off at high  $z$  – with a drop in their space density of only a factor  $\sim 2$  between  $z \sim 2$  and  $z \sim 4.4$  – when compared with the less luminous ones. Even though the lack of information on the behaviour of optically faint quasars at  $z \gtrsim 2.2$  does not allow any definitive conclusion, our results indicate the cosmological evolution of radio activity in quasars to be a function of their optical power.

## 8 ACKNOWLEDGEMENTS

MC acknowledges the support of PPARC, on rolling grant no. PPA/G/O/2001/00482. AC and LD acknowledge the Italian MIUR for financial support.

## REFERENCES

Becker R.H., White R.L., Helfand D.J., 1995, *ApJ*, 450, 559  
 Bennett C.L., et al. 2003, *ApJ*, 583, 1  
 Best P. N., Kauffmann G., Heckman T. M., Brinchmann J., Charlot S., Ivezic Ž., White, S. D. M., 2005, *MNRAS*, 362, 25  
 Boyle B.J., Shanks T., Croom S.M., Smith R.J., Miller L., Loaring N., Heymans C., 2000, *MNRAS*, 317, 1014  
 Carilli C.L., Bertoldi F., Rupen M.P., Fan X., Strauss M.A., et al., 2001, *ApJ*, 555, 625  
 Cavaliere A. & Vittorini V., 2002, *ApJ*, 570, 114  
 Cirasuolo M., Magliocchetti M., Celotti A., Danese L., 2003a, *MNRAS*, 341, 993  
 Cirasuolo M., Celotti A., Magliocchetti M., Danese L., 2003b, *MNRAS*, 346, 447  
 Cirasuolo, M., Magliocchetti, M., Celotti, A., 2005a, *MNRAS*, 357, 1267  
 Cirasuolo, M., Shankar F., Granato G.L., De Zotti G., Danese L., 2005b, *ApJ*, 629, 816  
 Condon J.J., O'Dell S.L., Puschell J.J., & Stein W.A. 1981, *ApJ*, 246, 624  
 Croom S.M., Schade D., Boyle B.J., Shanks T., Miller L., Smith R.J., 2004, *ApJ*, 606, 126  
 De Zotti, G., Ricci, R., Mesa, D., Silva, L., Mazzotta, P., Toffolatti, L., González-Nuevo, J., 2005, *A&A*, 431, 893  
 Di Matteo T., Springel V., Hernquist L., 2005, *Nature*, 433, 604  
 Dunlop J.S. & Peacock J.A., 1990, *MNRAS*, 247, 19  
 Dunlop J.S., 1998, in Bremer M.N., et al., eds., *Observational Cosmology with the New Radio Surveys*. Kluwer  
 Dunlop J.S., McLure R.J., Kukula M.J., Baum S.A., O'Dea C.P., Hughes D.H., 2003, *MNRAS*, 340, 1095  
 Fabian A.C. 1999, *MNRAS*, 308, L39  
 Fan X., Strauss M.A., Schneider D.P., Gunn J.E., Lupton R.H., 1999, *AJ*, 118, 1  
 Fan X., Strauss M.A., Richards G.T., et al. 2001a, *AJ*, 121, 31  
 Fan X., Strauss M.A., Schneider D.P., et al. 2001b, *AJ*, 121, 54  
 Fan X., Hennawi J.F., Richards G.T., et al., 2004, *AJ*, 128, 515  
 Ferrarese L. & Merritt D., 2000, *ApJ*, 539, L9  
 Granato G.L., Silva L., Monaco P., Panuzzo P., Salucci P., De Zotti G., Danese L., 2001, *MNRAS*, 324, 757  
 Granato G.L., De Zotti G., Silva L., Bressan A., Danese L., 2004, *ApJ*, 600, 580  
 Hasinger G., Miyaji T., Schmidt M., 2005, *A&A*, 441, 417  
 Hewett P.C., Foltz C.B., Craig B., Chaffee F.H., 1995, *AJ*, 109, 1498  
 Hewett P.C., Foltz C.B., Chaffee F.H., 2001, *AJ*, 122, 518  
 Ho L. C., 2002, *ApJ*, 564, 120  
 Jackson C.A. & Wall J.V., 1999, *MNRAS*, 304, 160  
 Jarvis M.J., Rawlings S., 2000, *MNRAS*, 319, 121  
 Jarvis M.J., et al. 2001, *MNRAS*, 327, 907  
 Jarvis M.J. & McLure R.J., 2002, *MNRAS*, 336, 38  
 Kellermann K.I., Sramek R., Schmidt M., Shaffer D.B., Green R., 1989, *AJ*, 98, 1195  
 Laor A., 2000, *ApJ*, 543, L111  
 Magorrian J., Tremaine S., Richstone D., Bender R., Bower G., Dressler A., Faber S. M., Gebhardt K., Green R., Grillmair C., et al. 1998, *AJ*, 115, 2285  
 Marshall H.L., 1987, *ApJ*, 316, 84  
 Marziani P., Zamanov R.K., Sulentic J.W., Calvani C., 2003, *MNRAS*, 345, 1133  
 McLure R.J. & Dunlop J.S., 2002, *MNRAS*, 331, 795  
 McLure R.J. & Dunlop J.S., 2004, *MNRAS*, 352, 1390  
 McLure R.J. & Jarvis M.J., 2004, *MNRAS*, 353, L45  
 Miller L., Peacock J.A., Mead A.R.G., 1990, *MNRAS*, 244, 207  
 Oshlack A. Y. K. N., Webster R. L., Whiting M. T. 2002, *ApJ*, 576, 81  
 Pentericci, L., et al., 2003, *A&A*, 410, 75  
 Schmidt M., 1968, *ApJ*, 151, 393  
 Schmidt M., van Gorkom J.H., Schneider D.P., Gunn J.E., 1995, *AJ*, 109, 473  
 Shaver P.A., Wall J.V., Kellermann K.I., Jackson C.A., Hawkins M.R.S., 1996, *Nature*, 384, 439  
 Shaver P.A., Windhorst R.A., Madau P., de Bruyn A.G., 1999, *A&A*, 345, 380  
 Silk J. & Rees M.J., 1998, *A&A*, 331, L1  
 Sramek R.A. & Weedman D.W., 1980, *ApJ*, 238, 435  
 Toffolatti L., Argueso Gomez F., De Zotti G., Mazzei P., Franceschini A., Danese L., Burigana C., 1998, *MNRAS*, 297, 117  
 Tremaine S., et al. 2002, *ApJ*, 574, 740  
 Ueda Y., Akiyama M., Ohta K., Miyaji T., 2003, *ApJ*, 598, 886  
 Vigotti M., Carballo R., Benn C.R., De Zotti G., Fanti R., Gonzalez Serrano J.I., Mack K-H., Holt J., 2003, *ApJ*, 591, 43  
 Woo J-H & Urry C.M., 2002a, *ApJ*, 579, 530  
 Woo J-H & Urry C.M., 2002b, *ApJ*, 581, L5  
 York D., et al. 2000, *AJ*, 120, 1579